Author version: J. Geophys. Res. (D: Atmos.), vol.115(16); 2010; doi:10.1029/2009JD013268, 12 pp

A century of climate variability in the central Dronning Maud Land, East Antarctica and its relation to Southern Annular Mode and El Niño Southern Oscillation

Sushant S. Naik[1,2*], Meloth Thamban [1], C. M. Laluraj[1], B. L. Redkar[1] and Arun Chaturvedi[3]

*1: National Centre for Antarctic and Ocean Research, Vasco-da-Gama, Goa, India 403804 (*sushant@nio.org)*

2:Natioanl Institute of Oceanography, Dona paula, Goa, India 403004

3: *Geological Survey of India (Antarctica Division), NH-5P, NIT, Faridabad, India 121001*

ABSTRACT

Stable isotope records of oxygen and hydrogen were studied from a 65 m long ice core retrieved from the central Dronning Maud Land, East Antarctica, in order to reconstruct the coastal Antarctic climate variability during the last century and its relation to the Southern Annular Mode (SAM) and El Niño Southern Oscillation (ENSO). The δ^{18}O records showed a significant relation to the SAM with a dominant ~4 years variability, except during specific periods (1918-1927; 1938-1947; 1989-2005) when ENSO teleconnection was established through the in-phase relation between SAM and Southern Oscillation Index (SOI). The combined influence of ENSO and SAM was seen on surface air temperatures in this region mainly during the austral summer season from 1989 to 2005. Further, a significant relationship between δ^{18}O and SAM was observed on a decadal scale, which overrides the intermittent influence of ENSO. Major shifts in the deuterium excess record were observed during periods of ENSO teleconnections, which support a shift in moisture source regions during the periods of stronger ENSO teleconnections. Surface air temperatures estimated using the δ^{18}O-T spatial slope for this region, depicted a significant warming of 1°C for the past century. The study reveals that throughout the last century, SAM was the dominant mode of climatic variability in the coastal region of central Dronning Maud Land on a decadal scale.

INTRODUCTION

Recent climate change in Antarctica is poorly understood due to the limited availability of instrumental data, coupled with the remoteness of the region. Although meteorological parameters are being measured at several stations along the coastal regions of Antarctica, these measurements started only in the late 1950s. For understanding the Antarctic climate variability, it is critical to have longer records from spatially distinct regions. These can be provided by ice cores, but are generally not available in a resolution comparable to the instrumental data. Using oxygen and hydrogen isotopes of snow it is possible to reconstruct past environmental variability, since a linear relationship exists between stable oxygen ($\delta^{18}O$) and hydrogen (δD) isotope values of snow and mean annual surface air temperature at the deposition site [*Dansgaard*, 1964]. But, this linear relationship is known to vary with space and time [e.g. *Jouzel et al.,* 1997]. Several factors have been reported to influence the isotopic composition of snow, such as: changing conditions in water vapour source regions, changes in magnitude of the ratio between advective and turbulent transport, changes in the strength of inversion layer, variations in the distillation history of air masses bringing precipitation to the core site, microphysical processes in clouds during snow formation, seasonality in precipitation and post-depositional isotopic diffusion [*Helsen et al.*, 2005 and references therein]. Further, wind-drifted snow from the Antarctic interior carried by katabatic winds as well as wind scouring could influence the isotopic records [*Fisher et al*., 1985; *Gregory and Noone*, 2008]. At coastal Antarctic sites, the isotopic content of snowfall is also sensitive to the sea ice extent [*Noone and Simmonds,* 2002; 2004]. Therefore, the use of oxygen and hydrogen isotopes of snow warrants a careful consideration of associated parameters and processes.

Large scale patterns of atmospheric circulation influence Antarctica to varying levels. On an inter-annual to decadal timescale, the Southern Annular Mode or Antarctic Oscillation (SAM/AAO) [*Thompson and Wallace*, 2000] and to a lesser extent the El Niño Southern Oscillation (ENSO) [*Bertler et al*., 2006], primarily drive the tropospheric Antarctic circulation. SAM is the principal mode of variability in the atmospheric circulation of the mid and high latitudes of the Southern Hemisphere, with synchronous anomalies of opposite sign in the mid and high latitudes [*Lefebvre et al.*, 2004]. It represents the periodical strengthening and weakening of the circumpolar vortex, which is the belt of tropospheric westerlies surrounding the Antarctic continent, and provides a means of coupling the Antarctic climate with that of lower latitudes [*Turner*, 2004]. During times of high SAM index, most of East Antarctica experiences cooling while the Antarctic peninsula experiences warming and strengthening of westerlies [*Kwok and Comiso*, 2002b]. ENSO, on the other hand, is characterised by a pattern of warm and cold sea surface temperature anomalies in the central and eastern equatorial Pacific with coupled atmospheric changes, which extend to Antarctica [*Turner*, 2004]. A study of inter-annual to decadal variability of SAM and ENSO in Antarctica and understanding of the mechanisms involved are expected to provide clues on Antarctic climate variability and its global implications. However, a critical requirement underlying the study of temporal variability of SAM and ENSO is the availability of highly resolved proxy records that go beyond the instrumental records.

Ice core studies with respect to climatic variability have been undertaken in the Dronning Maud Land (DML) region using deep [*EPICA Community Members*, 2006] and shallow [*Isaksson et al.*, 1996; *Isaksson et al.*, 1999; *Graf et al.*, 2002] ice cores. However, only a few high resolution ice core records are available from coastal regions of DML, that provide detailed evaluation of the environmental variability and its possible mechanisms [*Kaczmarska et al.*, 2004; *Divine et al.*, 2009]. The present study is an attempt to understand the influence of SAM and ENSO on the isotopic variability and the relationship between isotopes and surface air temperatures over the last century, using a high-resolution ice core record from the central DML region.

MATERIALS AND METHODS

The ice core IND-25/B5 (length: 65 m), analysed for the present study was retrieved during the 25th Indian Scientific Antarctic Expedition (2005-06) from the coastal ice sheet (location: 71° 20'S and 11° 35'E; elevation: ~1300m) in the central Dronning Maud Land (cDML) (Figure 1). Annual mean temperature at the core site and the accumulation rate reported in this area is ~ -20ºC and ~170 kg m^{-2} a^{-1}, respectively [*Anschütz et al.*, 2007]. The Ground Penetrating Radar (GPR) survey conducted prior to drilling as well as the available information [*Anschütz et al.*, 2007], indicated that the core site is not affected by glacial flow or any topographic undulations. Density of snow was estimated using weight and volume of the individual core sections, and the same was used to calculate the accumulation rates. Immediately after retrieval, the cores were labelled, stored under refrigeration (-20˚C) and shipped to Goa, India. The ice core samples were archived in frozen conditions until further processing. Prior to sub-sampling, the ice cores were manually decontaminated by removing a thin outer layer using microtome blades and sub-sampled at 5 cm intervals in the ice core processing facility (–15°C) at the National Centre for Antarctic and Ocean Research (NCAOR), Goa, India.

Stable isotope ratios of the melted ice samples were measured using an 'Isoprime' Isotope Ratio Mass Spectrometer (IRMS) (GV instruments, UK). Oxygen isotope ratios were determined by following the method of equilibrating the water samples with CO_2 gas [*Epstein and Mayeda*, 1953]. Hydrogen isotope analysis was done by following the method of H_2-H_2O equilibration using platinum catalyst [*Coplen et al.*, 1991]. All measurements were made against NIST standard reference materials, Vienna Standard Mean Ocean Water (VSMOW) and Standard Light Antarctic Precipitation (SLAP) [*Coplen*, 1996]. The isotopic composition is expressed in per mil (‰) as the deviation of a sample from the VSMOW standard. The external precision (1σ) obtained using a laboratory standard (CDML1) on oxygen and hydrogen was ± 0.05‰ and ± 0.77‰, respectively. Replicate analysis performed on ten samples yielded a repeatability of ± 0.05‰ and ± 0.8‰ on oxygen and hydrogen isotope, respectively. The estimated precision of deuterium excess values based on the precision of oxygen and hydrogen was ± 0.87‰.

The SAM data used in this study is a reconstructed index based on multiple linear regression of available station data from across the Southern Hemisphere, with the regression equation based on the statistical relationship of the principal components from the group of stations to a predictor [*Jones et al.*, 2009]. The predictor in this case is a SAM index based on the first Empirical Orthogonal Function (EOF) of Southern Hemisphere extra-tropical sea level pressure, derived from the European Centre for Medium Range Weather Forecasts (ECMWF) ERA-40 reanalysis. The Southern Oscillation Index (SOI) was obtained from the Australian Bureau of Meteorology (http:// www.bom.gov.au/climate/current/soihtm1.shtml). The 'Novolazarevskaya' station surface air temperature (SAT) as well as relative humidity record were obtained from the READER (REference Antarctic Data for Environmental Research) database and is available for the period from 1962 to present [*Turner*, 2004]. Correlations presented here between SOI, SAM and SAT were derived using the NCEP/NCAR reanalysis data [*Kalnay et al.*, 1996].

The age control for the IND-25/B5 ice core is based on multiple and complimentary methods: i) annual layer determination using the summer maxima in $\delta^{18}O$ values; ii) $nssSO_4^{2-}$ (non-sea salt sulphate) markers of volcanic eruptions; and iii) atomic bomb markers. The high sampling resolution ensured that each annual accumulation layer is represented on an average by thirteen $\delta^{18}O$ measurements. The topmost section of the core provides an average of fourteen samples per year for the last five years whereas the bottom section is characterised by eleven samples per year for the last five years. A five point smoothing was used for the entire $\delta^{18}O$ profile so as to facilitate the summer layer counting. Visual observations on a light table revealed the absence of any melt features in the ice core. Chronology of the ice core, determined by counting the seasonal cycles in the oxygen isotope data was further supported by the presence of $nssSO_4^{2-}$ peaks from the well-known Pinatubo (AD 1991) and Azul (AD 1932) volcanic eruptions. Annual $\delta^{18}O$ values were calculated from the unsmoothed data coincident with the calendar year. To further augment the dating procedure and confirm the preservation of upper layers, the tritium concentrations were measured on an annual basis from a selected section in the core. Tritium measurements were carried out on a liquid scintillation counter 'LKB Wallac Quantulus 1220', at the Low-Level Tritium Laboratory at Bhabha Atomic Research Centre (BARC, Mumbai, India). An increase in tritium level was found during the period 1962-1965, comparable to records from world over, resulting from nuclear testing activities in the early 1960s [*Jouzel et al.*, 1979]. Using such rigorous procedures, the core was dated back to the year 1905 with an error of ± 2 years (Figure 2a).

RESULTS AND DISCUSSION

The $\delta^{18}O$ values showed clear summer maxima and winter minima throughout the core, with values ranging from -20 to -37‰ whereas δD values ranged from -150 to -293‰ (Figure 2a). For the entire length of ice core presented here, the relationship between the oxygen and hydrogen isotopes followed the meteoric waterline [*Craig*, 1961] defined by $\delta D = 8.2*\delta^{18}O + 10.4$ ($r = 0.95$; $df = 1297$).

Annual accumulation rates at the core site calculated based on the summer peaks in $\delta^{18}O$ record (1905-2005) and density of snow at respective section, ranged from 110 kg m^{-2} a^{-1} to 528 kg m^{-2} a^{-1} (Figure 2b). The accumulation rates showed large variability with a standard deviation of ± 95 kg m^{-2} a^{-1}. Snow accumulation data, averaged for the DML region, provides values in the range of ~200-250 kg m^{-2} a^{-1} [*Vaughan et al.*, 1999*; Giovinetto and Zwally*, 2000]. Accumulation rate derived for the top snow section of the present core is ~290 kg m^{-2} a^{-1} and is comparable with earlier studies. Such high temporal accumulation variability is caused due to the large-scale variations in precipitation owing to cyclonic activities along the coastal areas of DML [*Schlösser and Oerter*, 2002].

In order to examine the extent to which the ambient air temperatures are represented by the isotopic composition of the snow, it is important to compare the $\delta^{18}O$ record with the measured air temperature from this region. Long-term meteorological data for this region is available from the coastal Russian station 'Novolazarevskaya' (Novo) (70° 46'S and 11° 50' E) which, however, is located at a much lower altitude (elevation ~100 m a.s.l) and ~65 km north of the core site, in the

Schirmacher Oasis. The precipitation and origin of moisture could be different at both locations, due to a significant difference in distance and elevation. Moreover, the presence of strong katabatic winds [*Parish and Bromwich*, 1987] could have an influence on snow redistribution. Therefore, the 'Novo' temperature record may only be a broad representation of the conditions prevailing at the core site. We examined the ice core annual δ^{18}O record for its relation to annual surface air temperature from 'Novo' for the period of data availability (1962 onwards). A poor positive correlation (r = 0.15, *df* = 44) between annual ice core δ^{18}O and annual 'Novo' surface air temperatures, suggests that processes other than temperature do influence the annual isotopic profile.

Relation between SAM, SOI, temperature and δ^{18}O records:

The SAM contributes to ~35% of variance in sea level pressure or geopotential height on a large range of time scales [*Marshall*, 2003]. It was observed that over the last 50 years the SAM has shifted into its positive phase, especially in summer and autumn, resulting in strengthening of the circumpolar westerlies and has significantly contributed to the spatial variability in Antarctic temperature change [e.g. *Thompson and Solomon*, 2002*; Kwok and Comiso*, 2002b; *Marshall*, 2003; *Schneider et al.*, 2004; *Turner et al.*, 2005]. This spatial variability was seen from the instrumental temperature data from coastal Antarctic stations which showed significant warming at western and northern parts of the Antarctic Peninsula and to some extent at 'Scott Base' [*Turner et al.*, 2005]. Conversely, a significant cooling was observed at 'Amundsen-Scott' in central Antarctica, whereas the rest of the continent did not show any discernible trend [*Turner et al.*, 2005]. Intriguingly, the station 'Novolazarevskaya' in the DML region of East Antarctica, displayed a warming trend for the entire period from 1962 to the present.

Further, to understand the relationship between annual δ^{18}O and SAM for the entire century, the ice core δ^{18}O record was compared with the reconstructed index of SAM for the period 1905 to 2005. Since the SAM is known to have a 4-5 yr variability [*Thompson and Wallace*, 2000], initially we applied a 4-year low pass filtering to the δ^{18}O record as well as to the SAM index (Figure 3a). The relationship between the two was insignificant and not stable in time (r = -0.1, *df* = ~25). Since, the SAM is also known to play an important role in driving decadal temperature changes [*Marshall*, 2006], we further examined the running decadal correlation between the annual δ^{18}O and SAM, which also revealed an insignificant relationship (Figure 3b). In East Antarctica, high polarity of SAM is known to correspond to lower temperatures and vice versa [*van den Broeke and van Lipzig*, 2004]. The oxygen isotopes taken as a temperature proxy should generally exhibit a negative relationship to SAM as revealed for East Antarctica [*Schneider et al.*, 2004]. Though the negative relationship was found to exist intermittently, during certain periods (1918-1927, 1938-1947 and 1989-2005), the correlation was found to diminish or become positive. It may be noted that uncertainties do exist in the SAM indices prior to 1957 when satellite data was not available and therefore relationships prior to 1957 remain inconclusive.

To further probe into the causal mechanisms for the temporal changes in correlations between annual δ^{18}O and SAM, we examined the temporal records of ENSO, which has a signature that extends to the mid and high latitudes in Southern Hemisphere. We utilised the reconstructed SOI, which is the normalized pressure difference between Tahiti (17.5^{o}S, 149.6^{o}W) and Darwin (12.4^{o}S, 130.9^{o}E), and used for reconstructing the ENSO. Several studies have shown that teleconnections exist between atmospheric conditions in the tropical Pacific and those at extra-tropical areas of the Southern Hemisphere [*Kwok and Comiso*, 2002a; *Yuan*, 2004; *Fogt and Bromwich*, 2006; *Gregory and Noone*, 2008]. The main connection of ENSO to Antarctica is believed to be through the Pacific South American pattern (PSA), which represents a series of positive and negative geopotential height anomalies initiated from tropical convection and extending from west-central equatorial Pacific to Australia, South Pacific near Antarctica, South America and then bending northwards toward Africa [*Karoly*, 1989]. Most importantly, ENSO is also known to affect the SAM, but in a highly non-linear way [*Turner*, 2004]. The two modes of climatic variability may combine, partially offset or enhance their influence on each other and on the Antarctic climate [*Bertler et al.*, 2006]. For the past century, we examined the relationship between the δ^{18}O record and the indices of SOI and SAM. The analysis showed that for the period wherein the δ^{18}O and SAM relationship was insignificant or positive (1918-1927, 1938-1947 and 1989-2005), the relationship between the SOI and SAM also tend to be in-phase (Figure 3b). An in-phase occurrence of SOI and SAM leading to strong ENSO teleconnections to Antarctica has been demonstrated recently [*Fogt and Bromwich*, 2006; *Gregory and Noone*, 2008]. These studies were mainly undertaken in the Pacific sector, where ENSO effect is dominant. *Divine et al.* [2009] studied a few ice cores from the coastal DML and suggested that ENSO teleconnections to this region occured only during certain periods and were caused due to bidecadal variability in SAM, forced by the tropical Pacific. The response of ice core δ^{18}O to the atmospheric circulation in all these studies was different due to the location of core site and biases in seasonal accumulation patterns.

Fogt and Bromwich [2006] reported that the austral spring (September, October, November; SON) and summer (December, January, February; DJF) best capture the influence of ENSO on Antarctica, since these are the seasons when ENSO matures. For a more recent period, an in-phase relationship between SAM and SOI was found during the austral spring and summer, which appears to be stronger during the 1990s [*Fogt and Bromwich*, 2006]. In the present study, the correlations between seasonal SAM as well as seasonal SOI and annual $\delta^{18}O$ record for the entire period from 1905 to 2005 were examined (Figure 3c). The running 10-year correlations between $\delta^{18}O$ and SAM showed dissimilar seasonal trends, with the spring SAM best resembling the running correlations between annual SAM and $\delta^{18}O$, followed by the summer SAM. The relationship as seen for the annual SAM and $\delta^{18}O$ was not stable in time, with diminished or positive correlations during the periods, 1918-1927, 1938-1947 and 1989-2005. In general, the correlations were negative as seen in the annual correlations; and weakened or were positive during the stated periods. In case of correlations between $\delta^{18}O$ and seasonal SOI, all the seasons displayed a similar variability. It was observed that throughout the last century, the $\delta^{18}O$/SOI running decadal correlation was opposite to that of the $\delta^{18}O$/SAM. During certain periods (1918-1927, 1938-1947 and 1989-2005), when the $\delta^{18}O$/SAM relationship was weakened, the SOI correlations with $\delta^{18}O$ were significantly negative. This indicates that during warm ENSO events, positive $\delta^{18}O$ anomalies were noticed in the study site and vice versa. Such a relation between SOI and $\delta^{18}O$ was also reported from the coastal DML [*Divine et al.*, 2009]. The above-mentioned intervals incorporate several El Niño and La Niña* years (1918, 1919, 1921*, 1923, 1924*, 1925; 1938*, 1940, 1941, 1943*, 1946; 1989*, 1991, 1993, 1994, 1997, 1998*, 1999*, 2002, and 2004, as determined from the SOI). When these years of El Niño and La Niña events were omitted from the record, the relationship between the 4-year low pass filtered $\delta^{18}O$ and SAM became statistically significant with a negative correlation (r = -0.45, *df* = ~20). Our analyses suggest that ENSO events weakened the SAM-temperature relationship during the specific intervals mentioned above when ENSO and SAM tended to be in phase. A combined influence of ENSO-SAM modes therefore, controlled the temporal changes in $\delta^{18}O$ at the core site. Such an interpretation is supported by the study of *Divine et al.* [2009] which demonstrated that at 2-6 year timescales, the ENSO did establish an intermittent teleconnection with the coastal DML region during the period 1955 to 1999.

The SAM-$\delta^{18}O$ association was further analysed using spectral analysis on the annual oxygen isotope time series, by means of the REDFIT 3.5 programme [*Schulz and Mudelsee*, 2002]. The power spectrum revealed statistically significant variability at ~4 years (95% significance level; Figure 4a) and is in agreement with the 4-5 year variability of the SAM [*Thompson and Wallace*, 2000]. Another less significant peak in the power spectrum of $\delta^{18}O$ was seen at ~6 years, which is attributable to ENSO and probably interferes with the low frequency variability, thus weakening the 4-year low pass filtered SAM-$\delta^{18}O$ relationship. In addition, the SAM index was observed to have a

~10 year variability, which was also seen in the $\delta^{18}O$ record of IND-25/B5 ice core, but did not exceed the significance level. We therefore examined the relationship between 8-12 year band pass filtered SAM and $\delta^{18}O$ data, which showed a significant negative correlation (r = -0.72, *df* = ~10) for the entire period (Figure 4b). Hence, the SAM dominates the isotopic (and temperature) variability in this part of East Antarctica on a decadal time scale in spite of the intermittent influence of ENSO.

To evaluate whether ENSO influences air temperatures at the study region, two distinct periods (1979-1989 and 1989-2005, wherein the relationship between SAM and $\delta^{18}O$ shifts from negative to positive, respectively) were studied in detail and the NCEP reanalysis data for this period was examined. The reason for selecting the year 1979 as the commencing year is that, from 1979 to the present, the NCEP data is reliable [*Turner*, 2004]. The relationship between SAM as well as SOI and surface air temperatures at the core location showed that SAM is negatively correlated to annual surface air temperatures from 1979 to 1989 (r = -0.6; *df* = 11; not shown). Significant relationship was also found between the winter air temperatures and SAM for the period 1979 to 1989 (r = -0.7; *df* = 11; not shown). A similar relation between the SAM index and winter air temperatures at 'Novo' has been reported earlier [*Marshall*, 2006]. During 1989-2005, the relation between SAM and surface air temperatures was insignificant on annual basis, but for the summer period, the relationship was significant (r = -0.5, *df* = 17, not shown). However, the relationship of SOI to annual surface air temperatures was found to be insignificant for the periods, 1979-1989 and 1989-2005. When the summer season was considered, the correlation between the two became statistically significant for the period 1989 to 2005 (r = -0.4, *df* = 17; not shown). The negative sign signifies that during the warm ENSO events, warmer temperatures are recorded at the coastal DML region and vice versa. We did not observe a significant relationship between SOI and surface air temperatures during the autumn. It is therefore suggested that the ENSO affects the air temperatures (hence the $\delta^{18}O$ values) of the coastal DML region particularly during the austral summer. The present study suggests that for the period of 1989-2005, both ENSO and SAM influenced the air temperatures during austral summer. Prior to this period (1979-1989), the SAM alone had a stronger influence on the air temperatures during austral winter for the central DML region. The connections between the ENSO and SAM appear only in the season when the ENSO phases reach their mature stage and the forcing is particularly strong, namely, the austral summer. During the austral summer, warm tropical Pacific sea surface temperatures (SST) resulting from warm ENSO events lead to negative phases of SAM [*Zhou and Yu*, 2004; *Fogt and Bromwich*, 2006; *L'Heureux and Thompson*, 2006].

During El Niño events, the PSA pattern gives rise to positive geopotential height anomalies over the Amundsen-Bellingshausen seas and negative anomalies over the Weddell Sea region. This phenomenon, referred to as the Antarctic Dipole, is reflected in the out-of-phase relationship between sea ice and surface temperature anomalies in South Pacific and South Atlantic [*Yuan*, 2004]. As a result, the cyclonic activity in the Weddell Sea intensifies during El Niño periods. In order to understand the typical air parcel route to the study area, 5 day back trajectory analyses were carried out at 500 hpa level above the drilling site, at every 6 hour interval during July 1997 (El Niño year) (Fig.5) using the National Institute for Polar Research trajectory model (NITRAM) [*Tomikawa and Sato*, 2005] and ERA-40 reanalysis data. July was selected as a representative period as *Suzuki et al.* [2008] have shown that throughout the year there is little difference in air parcel routes to the DML region. Our study indicates that the moisture is mainly derived from the Weddell Sea and the southern Atlantic Ocean, with a minor contribution from the Pacific Ocean. The cyclonic circulation of the Weddell Sea brings in warm air to the DML region. Previous studies have also made similar observations [*Noone et al.*, 1999; *Reijmer and van den Broeke*, 2001]. The moisture advection into the coastal region would be supplemented by the negative SAM, which leads to the weakening of westerlies. This would result in warm atmospheric air mass from lower latitudes to advect over Antarctica causing rise in surface air temperatures during austral summer, leading to a better teleconnection of ENSO to this region.

The reanalysis findings were further supported by correlating the temperature record from the 'Novo' station and the δ^{18}O record from the ice core. A weak positive correlation was observed between δ^{18}O and air temperatures in austral winter (r = 0.16, *df* = 44). Austral summer temperatures showed a significant positive correlation to the annual δ^{18}O (r = 0.25, *df* = 44) for the entire record from 1962 to 2005. During the other seasons (autumn and spring), no significant relationship was seen. When the individual months were considered for further analysis, January temperatures showed the most significant correlation (r = 0.39, *df* = 44) for the entire record from 1962 to 2005. Several studies have provided evidence of strong correlation between SAM and temperatures from 'Novo' during summer and autumn [*Turner et al.*, 2005; *Marshall*, 2006; *Visbeck*, 2007]. It is suggested that the weak winter δ^{18}O-temperature relationship is apparently due to post-depositional changes or due to the large interannual variability in precipitation.

Deuterium excess, $\delta^{18}O$ –T relationship and environmental implications:

The deuterium excess ($d = \delta D - 8 * \delta^{18}O$) parameter is generally used to infer information such as temperature and relative humidity of the moisture source areas [*Ciais et al.*, 1995*; Jouzel et* *al.*, 2003]. In general, higher deuterium excess values from polar ice cores reflect a more distant moisture origin while the lower deuterium excess indicates evaporation at higher latitudes [e.g.. *Vimeux et al.*, 1999]. However, the precipitation events in coastal regions are complex and it is more difficult to extract information of the moisture source conditions from deuterium excess alone. A recent study suggests that the deuterium excess parameter is mainly affected by the altitude of moisture transport trajectory [*Helsen et al.*, 2006].

In the present study, deuterium excess varied from -1.0 to 10.6‰ during 1905-2005, with an average value of 4.3‰. The large shifts in deuterium excess record correspond to periods when ENSO events influenced the δ^{18}O record (shaded regions in Figure 6). This suggests that the air trajectories in this region are influenced by the cyclonic activity as observed for the entire DML region [*Noone et al.*, 1999]. The main source of moisture in DML is considered to be the Weddell Sea region, which is known to be a cyclogenetic area [*Noone et al.*, 1999]. Cyclonic activity could substantially influence the air parcel paths and bring in warm moist air to the DML region. Further, we have analysed the relationship between the annual relative humidity values available from the 'Novo' station and annual deuterium excess data of IND-25/B5 ice core (Figure 6). A significant negative relationship was obtained (r = -0.26, *df* = 44), with higher relative humidity values at 'Novo' corresponding to lower deuterium excess in the ice core. Modelling studies have indicated an increase in deuterium excess of the vapour over the ocean surface with decreasing relative humidity and increasing ocean surface temperature [e.g., *Merlivat and Jouzel*, 1979]. However, in the present case, it is uncertain to what extent the relative humidity values are representative of the conditions over oceanic source area. While an air parcel travels over several days, it undergoes exchange of moisture by means of evaporation and precipitation with the surrounding boundary layer. Therefore, an air parcel can be associated with several moisture uptake locations, with the earliest evaporative sources contributing lesser to the precipitation at the arrival site [*Sodemann et al.*, 2008]. Considering the complexity of processes responsible for the changes in deuterium excess at coastal locations, we can only speculate that large variations in deuterium excess values are a consequence of shifting moisture source regions during the periods of stronger ENSO teleconnections.

The δ^{18}O records in the polar ice cores have often been used to determine the mean annual surface air temperatures at the site of precipitation using the δ^{18}O-T spatial slope [*Dansgaard*, 1964]. In East Antarctica, spatial variations in oxygen isotopes have been frequently used to determine the empirical relationship between the mean annual temperature and the δ^{18}O content in snow [*Isaksson and Karlén*, 1994 and references therein]. However, the application of spatial slope to temporal records is complicated by factors like, changes in the origin and transport of air masses, surface redistribution of snow and post-depositional changes in δ^{18}O arising from diffusion, which necessitate contemporaneous isotope and temperature measurements supported by borehole temperatures [*van Ommen and Morgan*, 1997]. Although borehole temperatures were not measured during the present study, the similarity between the 'Novo' summer temperature record (from 1962 onwards) and the ice core δ^{18}O record, suggests that the δ^{18}O record can provide a general surface air temperature trend for this region. Accordingly, the δ^{18}O–T spatial slope was applied to the present study, restricting the interpretation to long-term trend in temperature.

Studies conducted in the western DML provided spatial slopes ranging from 1.16 to 1.31‰ change in δ^{18}O/ºC with similar values for eastern DML [*Isaksson and Karlén*, 1994 and references therein]. The present core was retrieved from an area wherein not much information exists on the relationship between δ^{18}O and temperature. Therefore, an attempt was made to deduce an empirical relationship using the available information. *Masson-Delmotte et al.* [2008] considered a minimum of 200 samples within a radius of 400 km for this purpose. Since only a few studies are available in this region, thirteen sampling locations were chosen from a grid of ~71ºS to 76ºS and 5ºE to 15ºE (data from *Masson-Delmotte et al.*, 2008; Table 1)). Accordingly, the δ^{18}O-T plot provides a spatial slope of 1.31‰/ºC for this region. Using this deduced δ^{18}O-T spatial slope, we translated the ice-core δ^{18}O values to temperature, which gave an average temperature of -25.5°C for the period 1905-2005 (Figure 7). The average temperature at 'Novo' for the period 1962 to 2005 obtained from instrumental records was ~-10°C. Such large difference in annual air temperatures is expected on account of difference in altitude of the core site and the 'Novo' station. Accordingly, the temperature trend for the entire century showed a significant warming of 1°C or 0.1°C/decade. The 'Novo' station instrumental records also support a similar long-term temperature trend for the last ~50 years. *Steig et al.* [2009] have reported significant warming in East Antarctica at the rate of 0.1°C/decade for the period 1957–2006 and a continent-wide warming trend of 0.12°C/decade. Supporting evidence comes from another coastal ice core from DML (S100; Figure 1), which estimated a positive trend of 0.12‰/decade for a similar time period [*Divine et al*., 2009]. The present ice core study therefore, confirms a significant warming at DML during the past century (1905-2005).

CONCLUSIONS

We used an ice core, IND-25/B5 from the central DML region to understand the influence of two major modes of climate variability; SAM and ENSO on the isotopic variability as well as the relationship between oxygen isotopes and surface air temperatures in this region. The $\delta^{18}O$ record of the ice core, covering a period from 1905 to 2005, revealed a relation to SAM, which varied in time as observed in the annual as well as seasonal correlations between the two. An intermittent influence of ENSO was observed from the relationship between annual and seasonal SOI index on the $\delta^{18}O$ record at specific intervals (1918-1927, 1938-1947 and 1989-2005). It was further observed that during these specified intervals, the SAM and the SOI indices were in-phase, which indicates that the teleconnection of ENSO to the central DML occurs through the combined influence of SAM and ENSO. A significant negative relationship between SAM and the ice-core $\delta^{18}O$ record was observed only when the ENSO years occurring within the above mentioned intervals (1918-1927, 1938-1947 and 1989-2005) were eliminated. This negative relationship between SAM and the ice-core $\delta^{18}O$ indicates that the negative polarity of SAM leads to less negative $\delta^{18}O$ and warmer temperatures in the central DML, similar to the records from the East Antarctic region. On a decadal scale the SAM was seen to override the influence of ENSO on the $\delta^{18}O$ record.

As revealed by the NCEP reanalysis data for the period 1989-2005, the SAM and SOI indices showed a significant negative relationship with surface air temperatures, during the austral summer. This relationship between SOI and surface air temperature suggests that during an El Niño year within the period of 1989-2005, warmer air temperatures prevailed over the central DML. These evidences further support the finding that both the SAM and ENSO cause a combined influence on surface temperatures during austral summer in the central DML region.

The deuterium excess record of the ice core showed a significant relation to the relative humidity record from ‘Novo’. Our data revealed presence of major shifts in deuterium excess record for the years when the ENSO influenced the $\delta^{18}O$ record. This may indicate shifts in moisture source regions during the periods of stronger ENSO teleconnections. A significant warming trend of 1°C for the entire century was revealed in the SAT, which was estimated from the $\delta^{18}O$ record. This is also corroborated by the instrumental data from the ‘Novo’ station as well as earlier ice core records. This finding validates that the central DML is probably the only region in East Antarctica showing significant warming trend.

ACKNOWLEDGEMENTS

We thank the Ministry of Earth Sciences and Director, NCAOR for support. A. Rajakumar (NCAOR) and P. C. George (GSI) are acknowledged for their contribution in the field. We thank D. N. Sharma (Head, Radio Science and Safety Division), BARC, for extending the tritium analysis facility and Sonali and Priyanka for the tritium measurements. Thanks are also due to Yoshihiro Tomikawa (NIPR) for his help with the trajectory model and Karunakaran S. for preparation of the site map. Sincere thanks to the anonymous reviewers for their constructive suggestions.

REFERENCES

Anschütz, H., O. Eisen, H. Oerter, D. Steinhage, and M. Scheinert (2007), Investigating small-scale variations of the recent accumulation rate in coastal Dronning Maud Land, East Antarctica, *Ann. Glaciol*., *46*, 14–21.

Bertler, N.A.N., T.R. Naish, S. Kiphstuhl, P.J. Barrett, P.A. Mayewski, and K.J. Kreutz (2006), The effects of joint ENSO–Antarctic Oscillation forcing on the McMurdo Dry Valleys, Antarctica, *Antarct. Sci*., *18* (4), 507–514, doi: 10.1017/S0954102006000551.

Ciais, P., J.W.C. White, J. Jouzel, and J.R. Petit (1995), The origin of present-day Antarctic precipitation from surface deuterium excess data, *J. Geophys. Res*., *100*, D9, 18,917-18,927.

Coplen, T.B., J. D. Wildman, and J. Chen (1991), Improvements in the Gaseous Hydrogen-Water Equilibration Technique for Hydrogen Isotope ratio Analysis, *Anal. Chem*., *63* (9)*,* 910-912.

Coplen T.B. (1996), New guidelines for reporting stable hydrogen, carbon and oxygen isotope-ratio data, *Geochim. Cosmochim. Acta, 60*, 3359-3360.

Craig, H. (1961), Isotopic variations in meteoric waters, *Science*, *133*, 1702-1703.

Dansgaard,W. (1964), Stable isotopes in precipitation, *Tellus*, *16*, 436–468.

Divine, D. V., E. Isaksson, M. Kaczmarska, F. Godtliebsen, H. Oerter, E. Schlösser, S. J. Johnsen, M. van den Broeke, and R. S. W. van de Wal (2009), Tropical Pacific–high latitude south Atlantic teleconnections as seen in d18O variability in Antarctic coastal ice cores, *J. Geophys. Res*., *114*, D11112, doi:10.1029/2008JD010475.

EPICA Community Members (2006), One-to-one coupling of glacial climate variability in Greenland and Antarctica, *Nature*, *444*, 195-198.

Epstein, S., and T. Mayeda (1953), Variations of O^{18} contents of waters from natural sources, *Geochim. Cosmochim. Acta*., *4*, 213.

Fisher, D. A., N. Reeh, and H. B. Claussen (1985), Stratigraphic noise in time series derived from ice cores, *Ann. Glaciol*., *7*, 76–83.

Fogt, R. L., and D. H. Bromwich (2006), Decadal variability of the ENSO teleconnection to the high-latitude south Pacific governed by coupling with the southern annular mode, *J. Clim*., *19*, 979–997, doi:10.1175/ JCLI3671.1.

Giovinetto, M.B., and H.J. Zwally (2000), Spatial distribution of net surface accumulation on the Antarctic ice sheet, *Ann. Glaciol*., *31*, 171–178.

Graf, W., H. Oerter, O. Reinwarth, W. Stichler, F. Wilhelms, H. Miller, and R. Mulvaney (2002), Stable isotope records from Dronning Maud Land, Antarctica, *Ann. Glaciol*., *35*, 195–201.

Gregory, S., and D. Noone (2008), Variability in the teleconnection between the El Niño –Southern Oscillation and West Antarctic climate deduced from West Antarctic ice core isotope records, *J. Geophys. Res*., *113*, D17110, doi:10.1029/2007JD009107.

Helsen, M. M., R. S. W. Van de Wal, M.R. Van den Broeke, D. Van As, H.A.J. Meijer, and C.H. Reijmer (2005), Oxygen isotope variability in snow from western Dronning Maud Land, Antarctica and its relation to temperature, *Tellus*, *57B*, 423–435.

Helsen, M. M., R. S. W. van de Wal, M. R. van den Broeke, V. Masson-Delmotte, H. A. J. Meijer, M. P. Scheele, and M. Werner (2006), Modeling the isotopic composition of Antarctic snow using backward trajectories:Simulation of snow pit records, *J. Geophys. Res*., *111*, D15109,doi:10.1029/2005JD006524.

Isaksson, E and W. Karlén (1994), Spatial and temporal patterns in snow accumulation, western Droning Maud Land, Antarctica, *J. Glaciol*., *40* (135), 399-409.

Isaksson, E., W. Karlén, N. Gundestrup, P. Mayewski, S.Whitlow, and M.Twickler (1996), A century of accumulation and temperature changes in Dronning Maud Land, Antarctica, *J. Geophys. Res*., *101(D3)*, 7085-7094.

Isaksson, E., M. Van den Broeke, J.-G. Winther, L. Karlöf, J.-F. Pinglot, and N. Gundestrup (1999), Accumulation and proxy- temperature variability in Dronning Maud Land, Antarctica, determined from shallow firn cores, *Ann. Glaciol*., *29*, 17–22.

Jones, J. M., R. L. Fogt, M. Widmann, G. J. Marshall, P. D. Jones, and M. Visbeck (2009), Historical SAM Variability. Part I: century length seasonal reconstructions, *J. Clim*., doi:10.1175/2009JCLI2785.1.

Jouzel, J., L. Merlivat, M. Pourchet, and C. Lorius (1979), A continuous record of artificial tritium fallout at the South Pole (1954-1978), *Earth Planet. Sci. Lett*., *45*, 188-200.

Jouzel, J., R.B. Alley, M. Cuffey, W. Dansgaard, P. Grootes, G. Hoffman, S.J. Johnsen, R.D. Koster, D. Peel, C.A. Shuman, M. Stievenard, M. Stuiver, and J. White (1997), Validity of the temperature reconstruction from water isotopes in ice cores, *J. Geophy. Res*., *102*(C12), 26,471-26, 487.

Jouzel, J., F. Vimeux, N. Caillon, G. Delaygue, G. Hoffmann, V. Masson-Delmotte, and F. Parrenin (2003), Magnitude of isotope/temperature scaling for interpretation of central Antarctic ice cores, *J. Geophy. Res*., *108*(D12), 4361, doi:10.1029/2002JD002677.

Kaczmarska, M., et al. (2004), Accumulation variability derived from an ice core from coastal Dronning Maud Land, Antarctica, *Ann. Glaciol*., *39*, 339-345.

Kalnay, E., and co-authors (1996), The NCEP/NCAR 40-years reanalysis project, *Bull. Amer. Meteor. Soc.*, *77*, 437-470.

Karoly, D. J. (1989), Southern Hemisphere circulation features associated with El Niño–southern oscillation events, *J.*Clim., *2*, 1239–1252.

Kwok, R., and J. C. Comiso (2002a), Southern Ocean climate and sea ice anomalies associated with the Southern Oscillation, *J.Clim*., *15,* 487–501.

Kwok, R., and J. C. Comiso (2002b), Spatial patterns of variability in Antarctic surface temperature: connections to the Southern Hemisphere Annular Mode and the Southern Oscillation, *Geophys. Res. Lett*., *29*, 10.1029/2002GL015415.

Lefebvre, W., H. Goosse, R. Timmermann, and T. Fichefet (2004), Influence of the Southern Annular Mode on the sea ice–ocean system, *J. Geophys. Res.*, *109*, C09005, doi:10.1029/2004JC002403.

L'Heureux, M. L., and D. W. J. Thompson (2006), Observed relationships between the El Niño–Southern Oscillation and the extratropical zonal-mean circulation. *J. Clim*., *19*, 276–287.

Marshall, G.J. (2003), Trends in the Southern Annular Mode from observations and reanalyses, *J. Clim*., *16*, 4134–4143.

Marshall, G.J. (2006), Half-century seasonal relationships between the Southern Annular Mode and Antarctic temperatures, *Int. J. Climatol*., *27*, doi:10.1002/joc.1407.

Masson-Delmotte, V., et al. (2008), A Review of Antarctic Surface Snow Isotopic composition: Observations, Atmospheric Circulation, and Isotopic Modelling, *J. Clim*., *21*, 3359-3387.

Merlivat, L., and J. Jouzel (1979), Global climatic interpretation of the deuterium-oxygen 18 relationship for precipitation, *J. Geophys. Res*., *84*(C8), 5029– 5033.

Noone, D., J. Turner, and R. Mulvaney (1999), Atmospheric signals and characteristics of accumulation in Dronning Maud Land, Antarctica, *J. Geophy. Res*., *104*, D6, 19,191-19,211.

Noone, D., and I. Simmonds (2002), Annular variations in moisture transport mechanisms and the abundance of d18O in Antarctic snow, *J. Geophys. Res*., *107*(D24), 4742, doi:10.1029/2002JD002262, 2002.

Noone, D., and I. Simmonds (2004), Sea ice control of water isotope transport to Antarctica and implications for ice core interpretation*, J. Geophys. Res*., *109*, D07105, doi:10.1029/2003JD004228.

Parish, T. R., and D. H. Bromwich (1987), The surface windfield over the Antarctic ice sheets, *Nature*, *328*, 51-54.

Reijmer, C. H., and M.R. van den Broeke (2001), Moisture source of precipitation in Western Dronning Maud Land, Antarctica, *Ant. Sci*., *13*(2)*,* 210-220.

Schlösser, E., and H. Oerter (2002), Shallow firn cores from Neumayer, Ekstromisen, Antarctica: a comparison of accumulation rates and stable-isotope ratios, *Ann. Glaciol*., *35*, 91-96.

Schneider, D. P., E. J. Steig, and J. C. Comiso (2004), Recent climate variability in Antarctica from satellite-derived temperature data, *J. Clim.*, *17*, 1569–1583.

Schulz, M., and M. Mudelsee (2002), REDFIT: estimating red-noize spectra directly from unevenly spaced paleoclimatic time series, *Comp. Geosci.*, *28*, 421–426.

Sodemann, H., C. Schwierz, and H. Wernli (2008), Interannual variability of Greenland winter precipitation sources: Lagrangian moisture diagnostic and North Atlantic Oscillation influence, *J. Geophys. Res.*, *113*, D03107, doi:10.1029/2007JD008503.

Steig, E.J., D.P. Schneider, S.D. Rutherford, M.E. Mann, J.C. Comiso, and D.T. Shindell (2009), Warming of the Antarctic ice-sheet surface since the 1957 International Geophysical Year, *Nature*, *457*, 459-462, doi:10.1038/nature07669.

Thompson, D.W.J., and J. M. Wallace (2000), Annular modes in the extratropical circulation. Part I: month-to-month variability, *J. Clim.*, *13*, 1000–1016.

Thompson, D.W.J. and S. Solomon (2002), Interpretation of recent Southern Hemisphere climate change, *Science*, *296*, 895-899.

Tomikawa, Y. and K. Sato (2005), Design of NIPR trajectory model, *Polar Meteorol. Glaciol.*, *19*, 120-137.

Turner, J. (2004), Review: The El Niño–Southern Oscillation and Antarctica, *Int. J. Climatol.*, *24*, 1–31.

Turner, J., S. R. Colwell, G. J. Marshall, T. A. Laclan-Cope, A. M. Carleton, P. D. Jones, V. Lagun, P. A. Reid, and S. Iagovkina (2005), Antarctic climate change during the last 50 years, *Int. J. Climatol.*, *25*, 279-294.

van den Broeke, M. R., and N. P. M. van Lipzig (2004), Changes in Antarctic temperature, wind and precipitation in response to the Antarctic Oscillation, *Ann. Glaciol.*, *39*, 119– 126.

van Ommen, T.D., and V. Morgan (1997), Calibrating the ice core paleothermometer using seasonality, *J. Geophys. Res.*, *102* (D8), 9351-9357.

Vaughan, D.G., J.L. Bamber, M.B. Giovinetto, J. Russell, and A.P.R. Cooper (1999), Reassessment of net surface mass balance in Antarctica, *J. Clim.*, *12*(4), 933–946.

Vimeux, F., V. Masson, J. Jouzel, and M. Stievenard (1999), Glacial-interglacial changes in ocean surface conditions in the Southern Hemisphere, *Nature*, *398*, 410–413.

Visbeck, M. (2007), A station based Southern Annular Mode Index from 1885 to 2005, *J. Clim.*, *22* (4), 940-950.

Yuan, X. (2004), ENSO-related impacts on Antarctic sea ice: A synthesis of phenomenon and mechanisms, *Antarct. Sci.*, *16*(4), 415 – 425, doi:10.1017/S0954102004002238.

Zhou, T., and R. Yu (2004), Sea-surface temperature induced variability of the Southern Annular Mode in an atmospheric general circulation model, *Geophys. Res. Lett.*, *31*, L24206, doi: 10.1029/2004GL021473.

Table caption:

Table 1. Snow samples from the cDML region for deducing the δ-T slope.

Figure captions:

Figure 1. Map of central Dronning Maud Land showing location of ice core (IND-25/B5), Novolazarevskaya station and another coastal ice core (S100) used for comparison (see text).

Figure 2. a) The $\delta^{18}O$ profile (smoothed by 5 point running average) of core IND-25/B5 showing summer peaks in $\delta^{18}O$ along with the tritium profile of a section of the core (TU signifies Tritium Units), and b) Accumulation record from the IND-25/B5 ice core. Dotted line shows the long-term trend.

Figure 3. a) The 4 year low-pass-filtered data of ice core $\delta^{18}O$ and SAM index showing their inter-relationships. Shaded regions mark the years when correlations change. January temperatures from 'Novo' are plotted in comparison to $\delta^{18}O$ records; **b)** Running 10 year correlation between $\delta^{18}O$ and SAM, and SAM and SOI; **c)** Running 10 year correlation between seasonal SAM and $\delta^{18}O$ (upper panel) as well as SOI and $\delta^{18}O$ (lower panel). The 95% confidence levels are plotted as dotted lines at 0.54 and -0.54.

Figure 4. a) Power spectra of oxygen isotope record from core IND-25/B5. The dotted line is the background signal and the dashed line denotes the 95% significance level estimated using the chi square test (*n50*=1; Hanning window). b) 8-12 year band pass filtered data showing relation between $\delta^{18}O$ and SAM.

Figure 5. Horizontal and vertical trajectory distributions of the air parcels arriving at 500 hPa over the core site during July 1997.

Figure 6. Deuterium excess record of the ice core in comparison with the relative humidity data from 'Novo'. Shaded areas give the intervals of large shifts in deuterium excess record.

Figure 7. Temperature calculated using the $\delta^{18}O$-T spatial slope showing a warming trend.

Table 1. Snow samples from the cDML region for deducing the δ-T slope.

No.	CORE/SNOW SAMPLE ID	Latitude	Longitude	$\delta^{18}O$ (‰)	Temp (°C)	Reference
1	DML04C97_00	74.40°S	7.22°E	-47.11	-45.90	*Graf et al*., 2002
2	DML06C97_00	75.00°S	8.01°E	-47.45	-47.50	*Graf et al*., 2002
3	DML09S97_13	75.93°S	7.21°E	-48.30	-47.90	*Graf et al*., 2002
4	DML10C97_00	75.22°S	11.35°E	-49.05	-48.70	*Graf et al*., 2002
5	DML17C98_33	75.17°S	6.50°E	-46.35	-46.10	*Graf et al*., 2002
6	DML23C98_12	75.25°S	6.50°E	-46.76	-45.80	*Graf et al*., 2002
7	DML16C98_13	75.17°S	5.00°E	-45.08	-45.50	*Graf et al*., 2002
8	E	72.60°S	12.43°E	-25.71	-21.00	*Isaksson and Karlén*, 1994
9	G	73.04°S	5.06°E	-41.20	-40.10	*Isaksson et al*., 1999
10	I	73.72°S	7.94°E	-44.87	-44.60	*Isaksson et al*., 1999
11	K	74.35°S	11.10°E	-46.32	-47.80	*Isaksson et al*., 1999
12	L	74.65°S	12.79°E	-47.81	-49.30	*Isaksson et al*., 1999
13	M	75.00°S	15.00°E	-49.49	-51.30	*Isaksson et al*., 1999
14	POTSDAM GLACIER	71.08°S	11.59°E	-27.92	-20.00*	*Masson-Delmotte et al*., 2008

* Temperature value from *Anschutz et al*. [2007]

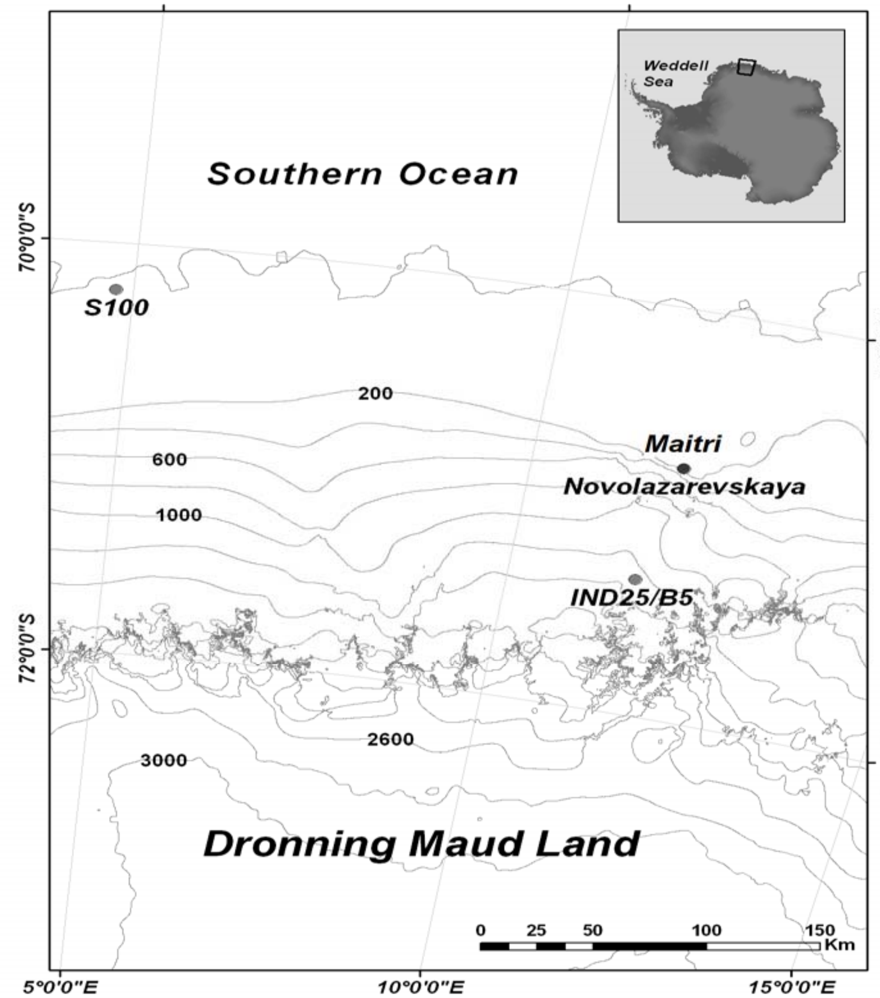
Weddell Sea
Southern Ocean
70°0'0"S
70°0'0"S
S100
200
Maitri
600
Novolazarevskaya
1000
IND25/B5
72°0'0"S
72°0'0"S
2600
3000
Dronning Maud Land
0
25
50
100
150
Km
5°0'0"E
10°0'0"E
15°0'0"E

Fig. 1

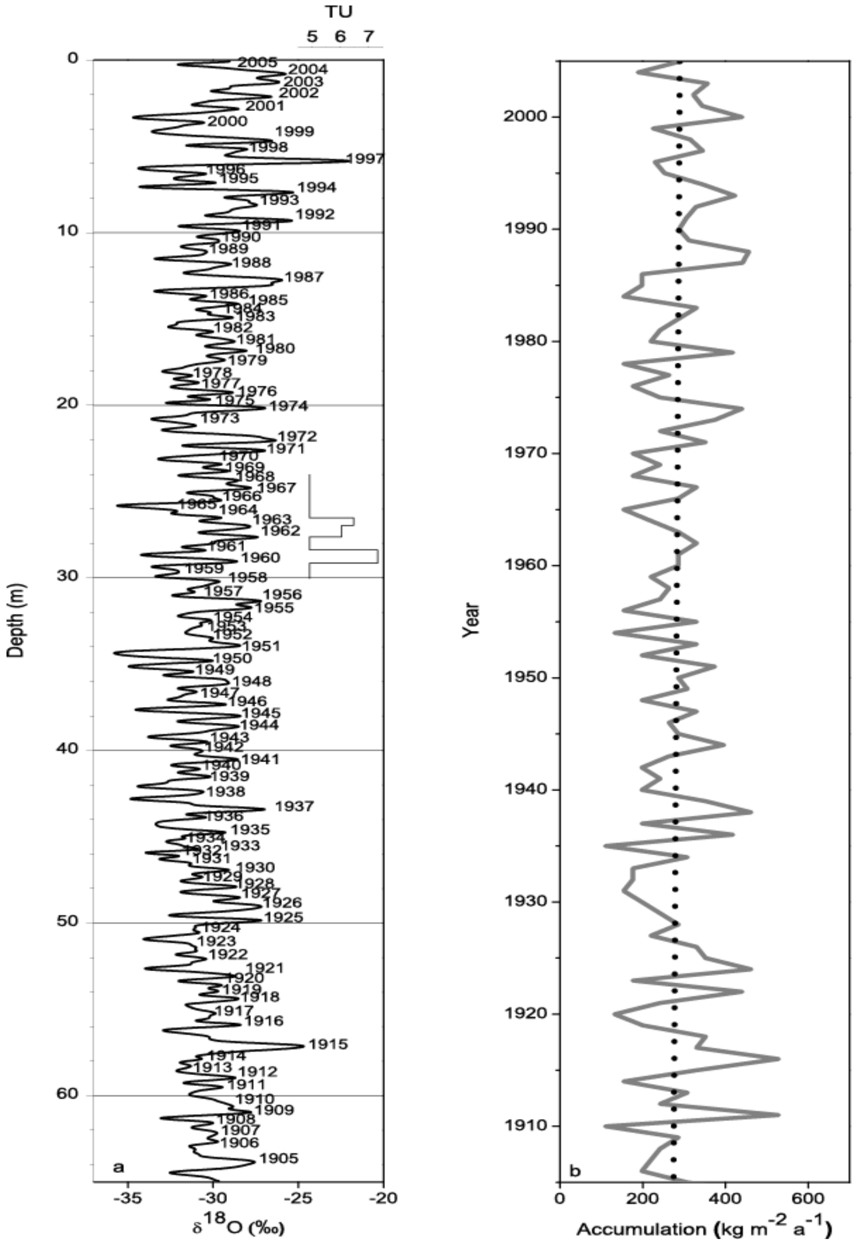
TU
5 6 7
Depth (m)
0
10
20
30
40
50
60
2005
2004
2003
2002
2001
2000
1999
1998
1997
1996
1995
1994
1993
1992
1991
1990
1989
1988
1987
1986
1985
1984
1983
1982
1981
1980
1979
1978
1977
1976
1975
1974
1973
1972
1971
1970
1969
1968
1967
1966
1965
1964
1963
1962
1961
1960
1959
1958
1957
1956
1955
1954
1953
1952
1951
1950
1949
1948
1947
1946
1945
1944
1943
1942
1941
1940
1939
1938
1937
1936
1935
1934
1933
1932
1931
1930
1929
1928
1927
1926
1925
1924
1923
1922
1921
1920
1919
1918
1917
1916
1915
1914
1913
1912
1911
1910
1909
1908
1907
1906
1905
a
-35
-30
-25
-20
δ^{18}O (‰)
Year
2000
1990
1980
1970
1960
1950
1940
1930
1920
1910
b
0
200
400
600
Accumulation (kg m^{-2} a^{-1})

Fig. 2

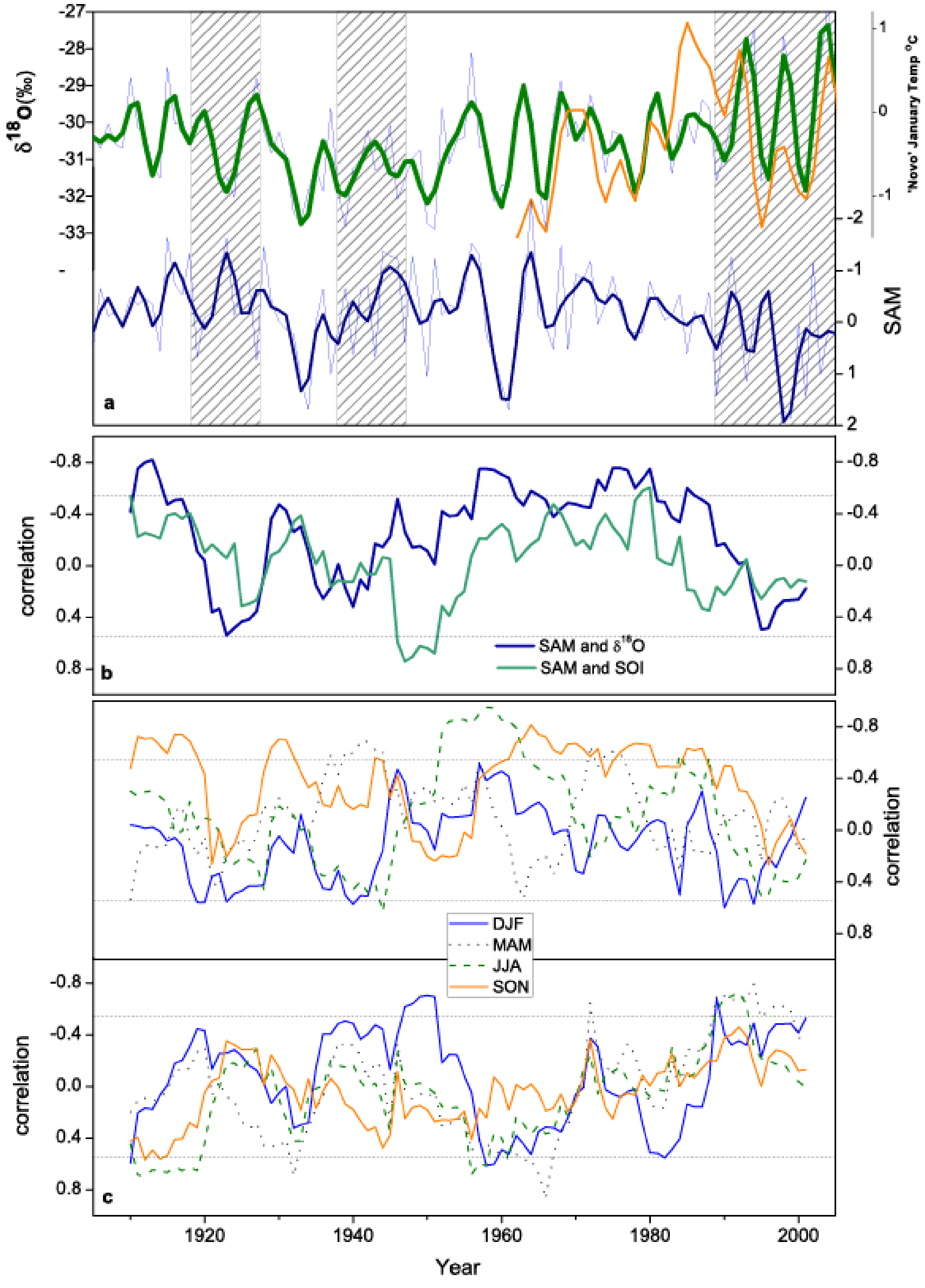

$\delta^{18}O$(‰)
-27
-28
-29
-30
-31
-32
-33
'Novo' January Temp °C
1
0
-1
-2
SAM
-1
0
1
2
a
correlation
-0.8
-0.4
0.0
0.4
0.8
SAM and δ^{18}O
SAM and SOI
b
DJF
MAM
JJA
SON
c
1920
1940
1960
1980
2000
Year

Fig. 3

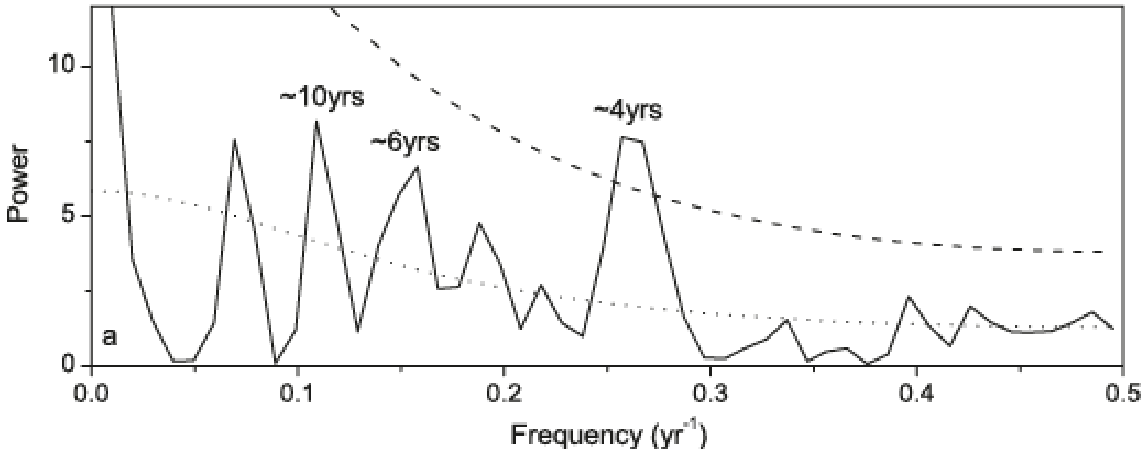
10
5
0
Power
~10yrs
~6yrs
~4yrs
a
0.0
0.1
0.2
0.3
0.4
0.5
Frequency (yr^{-1})

Fig.4a

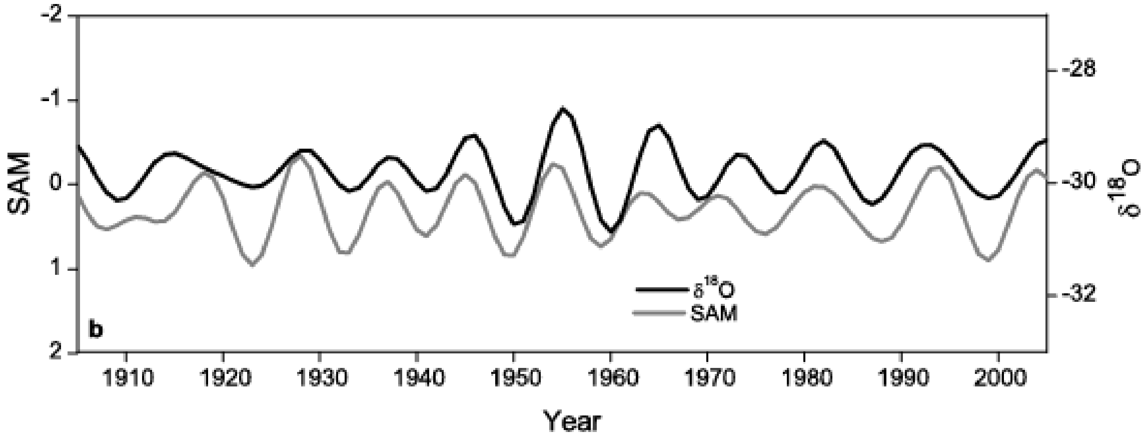
-2
-1
0
1
2
SAM
-28
-30
-32
$\delta^{18}O$
$\delta^{18}O$
SAM
b
1910
1920
1930
1940
1950
1960
1970
1980
1990
2000
Year

Fig. 4b

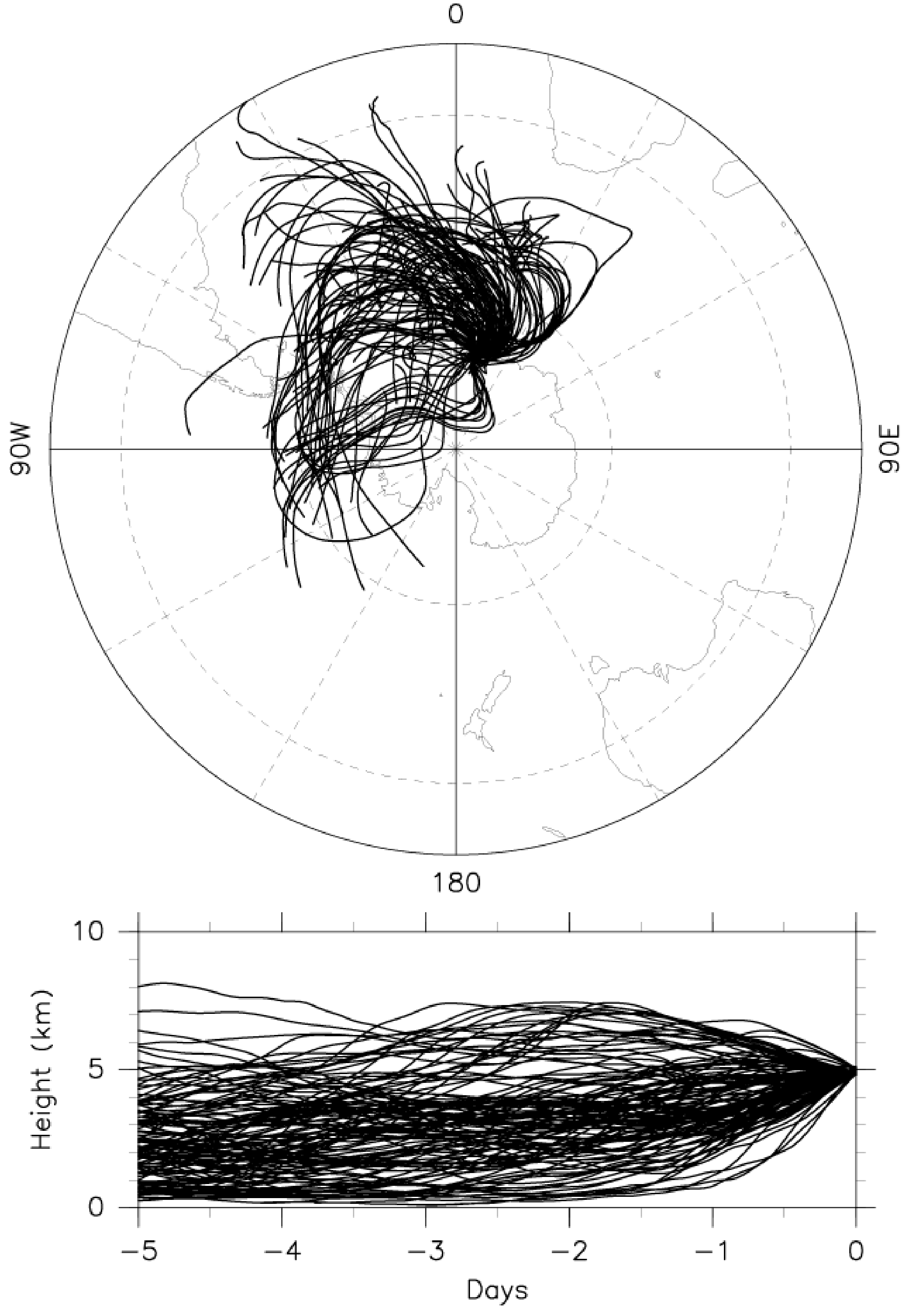

Fig. 5

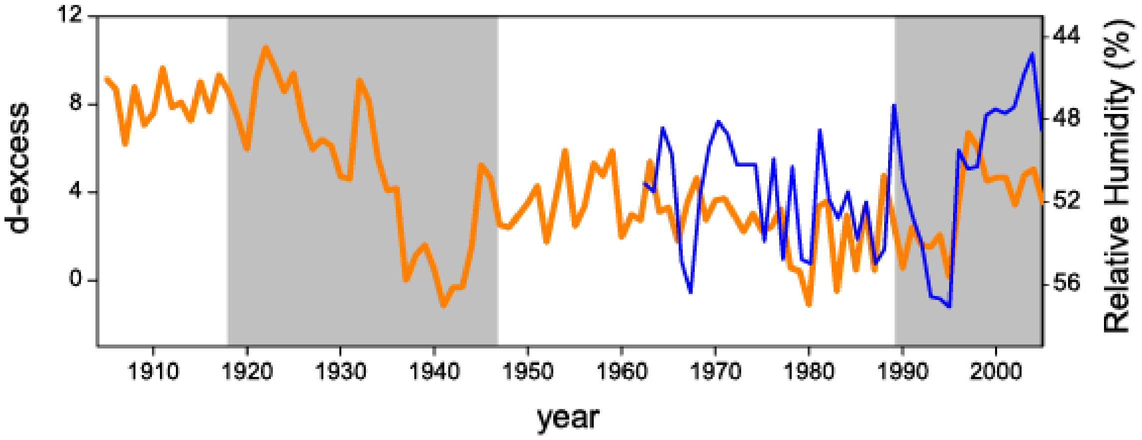
12
8
4
0
d-excess
44
48
52
56
Relative Humidity (%)
1910
1920
1930
1940
1950
1960
1970
1980
1990
2000
year

Fig.6

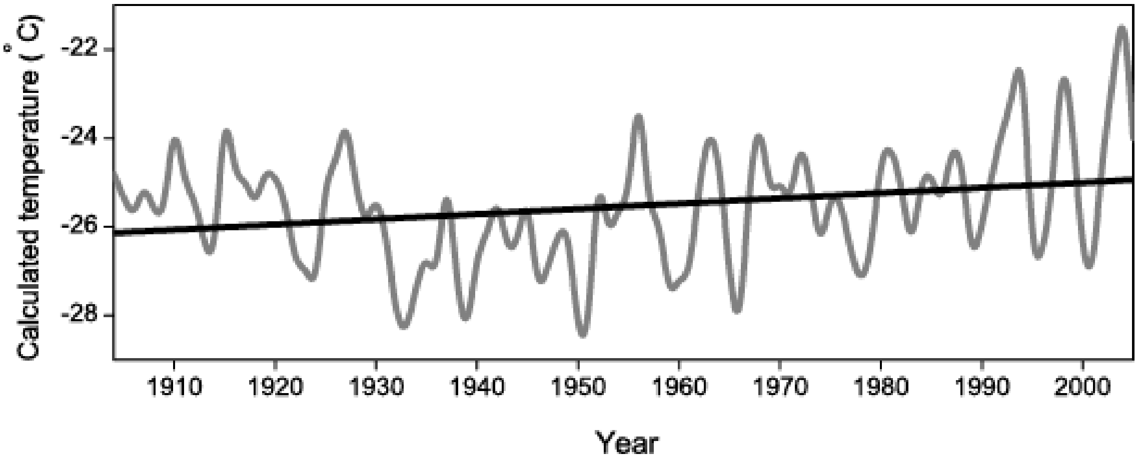
-22
-24
-26
-28
Calculated temperature (°C)
1910
1920
1930
1940
1950
1960
1970
1980
1990
2000
Year

Fig.7